

## Energy Flow and Stopping in Relativistic Heavy-Ion Collisions at $E_{\text{lab}}/A = 14.6$ GeV

J. Barrette,<sup>(3)</sup> R. Bellwied,<sup>(6)</sup> P. Braun-Munzinger,<sup>(6)</sup> W. E. Cleland,<sup>(5)</sup> G. David,<sup>(6)</sup> E. Duek,<sup>(1)</sup> M. Fatyga,<sup>(1)</sup> D. Fox,<sup>(2)</sup> A. Gavron,<sup>(2)</sup> S. V. Greene,<sup>(9)</sup> J. Hall,<sup>(4)</sup> T. K. Hemmick,<sup>(9)</sup> R. Heifetz,<sup>(7)</sup> M. Herman,<sup>(6)</sup> N. Herrmann,<sup>(6),(a)</sup> R. W. Hogue,<sup>(1)</sup> G. Ingold,<sup>(6)</sup> K. Jayananda,<sup>(5)</sup> D. Kraus,<sup>(5)</sup> D. Lissauer,<sup>(1)</sup> W. J. Llope,<sup>(6)</sup> A. Legault,<sup>(3)</sup> T. Ludlam,<sup>(1)</sup> R. Majka,<sup>(9)</sup> D. Makowiecki,<sup>(1)</sup> S. K. Mark,<sup>(3)</sup> J. T. Mitchell,<sup>(9)</sup> M. Muthuswamy,<sup>(6)</sup> E. O'Brien,<sup>(1)</sup> L. Olsen,<sup>(1),(a)</sup> V. Polychronakos,<sup>(1)</sup> M. Rawool-Sullivan,<sup>(8)</sup> F. Rotondo,<sup>(9)</sup> J. Sandweiss,<sup>(9)</sup> B. Shivakumar,<sup>(9)</sup> J. Simon,<sup>(8)</sup> U. Sonnadara,<sup>(5)</sup> J. P. Sullivan,<sup>(8)</sup> J. Stachel,<sup>(6)</sup> J. Sunier,<sup>(2)</sup> H. Takai,<sup>(1)</sup> T. Throwe,<sup>(1)</sup> H. Van Hecke,<sup>(2)</sup> L. Waters,<sup>(6)</sup> C. Woody,<sup>(1)</sup> K. Wolf,<sup>(8)</sup> and D. Wolfe<sup>(4)</sup>

(E814 Collaboration)

<sup>(1)</sup>Brookhaven National Laboratory, Upton, New York 11973

<sup>(2)</sup>Los Alamos National Laboratory, Los Alamos, New Mexico 87545

<sup>(3)</sup>McGill University, Montreal, Canada H3A 2T8

<sup>(4)</sup>University of New Mexico, Albuquerque, New Mexico 87131

<sup>(5)</sup>University of Pittsburgh, Pittsburgh, Pennsylvania 15260

<sup>(6)</sup>State University of New York, Stony Brook, New York 11794

<sup>(7)</sup>University of Tel Aviv, Tel Aviv, Israel

<sup>(8)</sup>Texas A&M University, College Station, Texas 77843

<sup>(9)</sup>Yale University, New Haven, Connecticut 06511

(Received 27 October 1989)

Collisions of  $^{28}\text{Si} + \text{Al, Cu, Pb}$  at  $E_{\text{lab}}/A = 14.6$  GeV were studied in a calorimetry-based experiment at the BNL Alternating Gradient Synchrotron. Transverse-energy production was measured for pseudorapidities  $-0.5 < \eta < 0.8$ . Correlations with the spectra and multiplicity of neutrons and protons emitted into a forward  $0.8^\circ$  cone demonstrate quantitatively the large amount of nuclear stopping observed in these reactions. Calculations in hadronic-fireball or nucleon-nucleon based models underpredict the measured transverse-energy production for Si+Pb and indicate the need to include rescattering of secondaries and/or contributions from target fragmentation.

PACS numbers: 25.70.Np

In collisions between relativistic heavy ions the question of stopping, i.e., energy loss of the projectile in a target nucleus, is of central interest. It determines the energy and baryon density achieved in the collision and is therefore of relevance for a possible formation of a thermalized quark-gluon plasma. Global quantities such as transverse energy  $E_T$  measured in a large acceptance detector, or forward energy measured in a small cone angle centered about the beam axis, have been accepted as empirical, model-dependent measures of stopping. Over the last two years, the first results of such measurements have become available. At BNL Alternating Gradient Synchrotron (AGS) energies<sup>1,2</sup> (10 and 14.6 GeV/nucleon) data on  $E_T$  production cover basically the forward hemisphere in the center-of-mass (c.m.) frame,  $1.2 < \eta < 3$ ; at CERN Super Proton Synchrotron energies<sup>3-5</sup> (60 and 200 GeV/nucleon) the range is  $-0.1 < \eta < 5.5$ , using the pseudorapidity  $\eta = \ln[\cot(\theta/2)]$ . In all of these experiments, transverse-energy production has been found to be large and clearly anticorrelated with forward energy. Therefore, a large amount of nuclear stopping has been inferred (see, e.g., Ref. 6), albeit in a model-dependent way. A crucial test of these models is a measurement of the spectra and multiplicity of forward-going nucleons as functions of the centrality of the reaction, as determined from  $E_T$  measurements. We

report, in this Letter, the first measurement of such neutron and proton spectra. Using these spectra we can define the stopping probability as  $p_S(E_T) = 1 - \langle M(E_T, y_b \pm \Delta y) \rangle / A_P$ . Here,  $\langle M \rangle$  is the mean multiplicity of nucleons found within the interval  $\Delta y$  of beam rapidity  $y_b = 3.44$  at 14.6 GeV/nucleon and  $A_P$  is the projectile mass number. From Fermi motion in the projectile we estimate with Fermi momentum  $p_F = 0.27$  GeV/c that  $\Delta y = 1.17 \sinh^{-1}(p_F/m_{Nc}) \approx 0.34$ . Employing this stopping definition we demonstrate below that stopping is complete at AGS energies.

The experiment was performed using a  $^{28}\text{Si}$  beam of the BNL AGS at  $E_{\text{lab}}/A = 14.6$  GeV of intensity  $5 \times 10^4$ /sec to bombard targets of Al, Cu, and Pb, with thicknesses corresponding to 1.2% of a nuclear interaction length. The integrated luminosity reached 0.2/ $\mu\text{b}$  for each target. The E814 experimental apparatus is sketched in Fig. 1. Energy flow is measured in the target calorimeter. The participant calorimeter, which was not instrumented at the time, served as a  $2.0 \times 2.4$ -in.<sup>2</sup> collimator corresponding to approximately a  $0.8^\circ$  opening angle centered about the beam direction. Particles passing through this opening are measured in the forward spectrometer. The total distance from target to downstream calorimeters is about 36 m (note the break in the scale in Fig. 1). Detectors from which data are present-

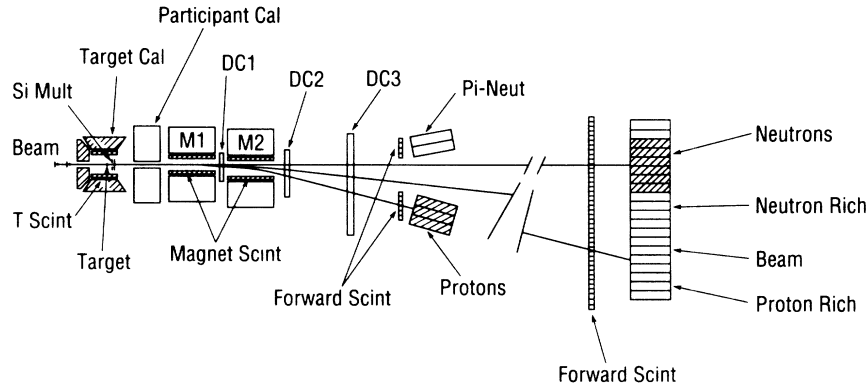


FIG. 1. Schematic drawing of the E814 experimental apparatus (not to scale).

ed in the present analysis are shaded in Fig. 1 and will be briefly described here.

The target calorimeter (T Cal) is a device consisting of 992 NaI crystals each 13.8 cm deep, corresponding to 5.3 radiation lengths or  $\frac{1}{3}$  of a nuclear interaction length. They are arranged in an approximate projective geometry in five walls, four parallel to the beam at  $-0.5 < \eta < 0.8$  and one perpendicular as a backwall ( $-2 < \eta < -0.9$ ). Each NaI crystal is read out with a vacuum photodiode through an amplifier chain. The average noise in a channel corresponds to  $\sigma_E = 1.7$  MeV of which about 1 MeV is correlated in all channels. The calibration is performed using cosmic rays. The inside of the target calorimeter is lined with 52 plastic-scintillator paddles arranged parallel to the beam and used to derive an interaction trigger. Charged-particle multiplicities are measured in a pair of Si-pad detectors, each with 512 pixels and together covering  $1.3 < \eta < 4.0$ . Particles emitted into  $\theta < 0.8^\circ$  traverse a magnetic field ( $M1$ ,  $M2$ ) of integrated flux 6 Tm corresponding to a  $p_T$  kick of about  $1.8$  GeV/ $c$  for singly charged particles. Protons with kinetic energies between about 10 and 15 GeV are detected in three U-Cu-scintillator sampling calorimeters<sup>7</sup> labeled "protons" in Fig. 1. Each calorimeter module has a cross-sectional area of  $20 \times 120$  cm<sup>2</sup> and is read out in optically decoupled towers of  $10 \times 20$  cm<sup>2</sup>, each viewed by two photomultipliers. The calorimeter depth corresponds to about 4.2 interaction lengths. Neutrons are detected in a set of six identical calorimeter modules 36 m downstream of the target. The hadronic-energy resolution of these calorimeters was measured<sup>7</sup> to be  $\Delta E/E = 0.37/[E \text{ (GeV)}]^{1/2}$ ; the typical noise of one readout channel is 100 MeV. Each forward-energy measurement is complemented by a charge measurement in vertical scintillator paddles ("forward scintillators" in Fig. 1, dimensions  $10 \times 120 \times 1$  cm<sup>3</sup>).

The data presented here were taken using four parallel triggers downscaled to run at comparable rates: an interaction trigger (pretrigger) requiring a small number of hits in the target scintillators or the Si multiplicity counters and three different levels of  $E_T$  in the T Cal. The  $E_T$  triggers were obtained by splitting the T Cal sig-

nals and performing fast analog sums with the appropriate  $\sin(\theta)$  weights. Background in the spectra resulted mainly from upstream interactions,  $\delta$ -electron production in the target leading to spurious pretriggers, or random beam coincidences. These backgrounds were quantitatively rejected. Uncertainties in this rejection are well within the statistical error bars shown in Fig. 2.

Figure 2 shows the resulting  $E_T$  spectra measured in the sidewalls of the T Cal ( $-0.5 < \eta < 0.8$ ). The data in Fig. 2 have not been corrected for leakage, which is substantial due to the limited depth of the NaI crystals. We have, however, tracked through the target-calorimeter particles from Monte Carlo event generators based on the Landau-hydrodynamical model<sup>6</sup> and on HIJET<sup>8,9</sup> using the GEANT package.<sup>10</sup> The results include folding with the experimental noise and are also shown in Fig. 2. To illustrate the size of the correction, the solid lines in Fig. 2 show the primary  $E_T$  distributions of the Landau model into the T Cal acceptance, the dashed lines indicate how much of this energy should actually be observed in the T Cal; this is about  $\frac{1}{2}$  of the primary transverse energy for the Pb target and somewhat more, because of the relative increase of the noise contribution, for the lighter targets. Very similar leakage correction factors are obtained if one uses HIJET as the event generator (see top panel of Fig. 2). The observed  $E_T$  values show a strong increase with increasing target mass. This trend becomes even more pronounced if one takes into account the target dependence of the ratio between measured and primary transverse energy. Such behavior is qualitatively expected due to both the slowing down of the fireball c.m. motion with increasing target mass and the increasing importance of rescattering and target spectator fragments.

The large amount of transverse energy produced in the backward-angle region covered by the T Cal should also be reflected in the shape of spectra of leading baryons in central collisions. To study quantitatively the forward baryon spectra we have performed an analysis of the baryons in the forward  $0.8^\circ$  cone, based on the (kinetic) energy they deposit in the calorimeters of the forward spectrometer and on the absence (presence) of a mini-

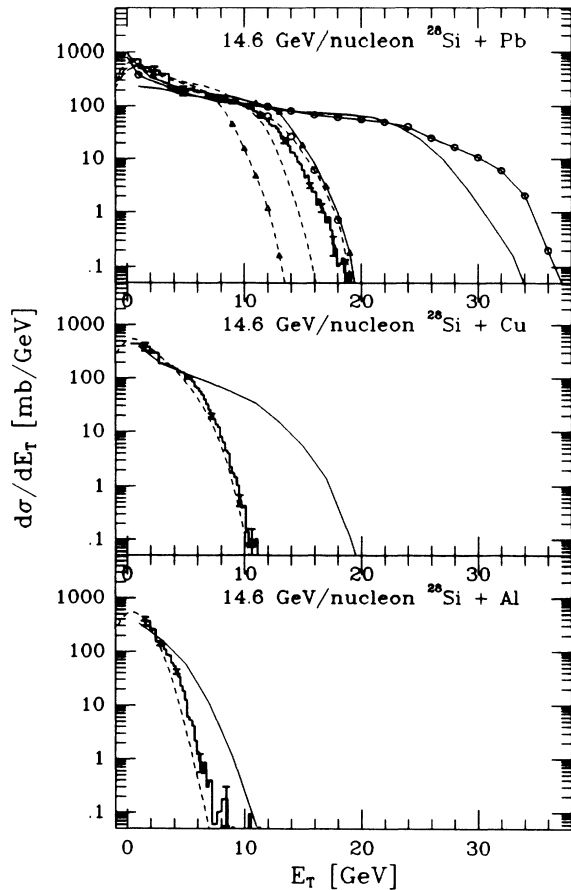


FIG. 2. Experimental transverse-energy spectra as measured by the TCal,  $-0.5 < \eta < 0.8$ . Solid lines:  $E_T$  from various models into the TCal acceptance, Landau fireball (line without symbols), HIJET without rescattering (Ref. 8) (triangles), and HIJET with rescattering (Ref. 9) (open circles). Dashed lines: Same as solid lines, but corrected for leakage and resolution.

imum ionizing signal in the forward scintillators for neutrons (protons). Since the analysis of protons is restricted, due to the magnetic field, to  $T > 10$  GeV, we do not expect any contamination from pions in the proton sample (a pion of beam rapidity  $y_b = 3.44$  deposits 2.2 GeV in the calorimeter). The neutral-particle sample in the energy range  $> 1.5$  GeV consists overwhelmingly of neutrons. Photons originating from the decay of  $\pi^0$  mesons produced in the target are completely negligible because of the small ( $< 1$  msr) solid angle through the participant calorimeter. The background due to secondary interactions of beam-rapidity nucleons downstream of the target was estimated by tracking nucleons hitting the participant calorimeter and/or magnets using GEANT.<sup>10</sup> For  $1.5 < T < 12.5$  GeV the biggest source of background is secondary neutrons. Their rate is, however, well within the experimental error bars and amounts, e.g., to 2% of the data for the highest  $E_T$  bin.

We focus in the following on data for the Pb target. To identify single and multiple hits, the energy deposited

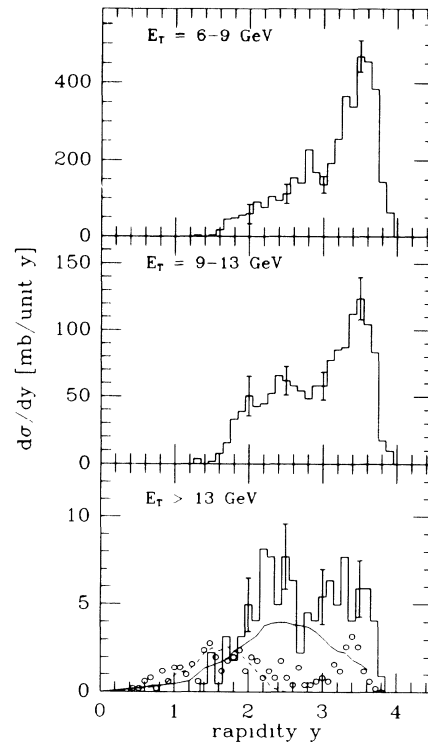


FIG. 3. Inclusive neutron-rapidity spectra measured in a forward  $0.8^\circ$  cone for 14.6 GeV/nucleon  $^{28}\text{Si} + \text{Pb}$  and different transverse energies in TCal. Experimental threshold 1.3 GeV. Open circles, HIJET (Ref. 9); dashed line, isotropic fireball (Ref. 6); solid line, Landau fireball (Ref. 6).

in the 144 channels of the neutron region (Fig. 1) was subject to a cluster analysis using a pattern recognition algorithm.<sup>7</sup> From the measured positions and energies one then obtains neutron-rapidity distributions. Figure 3 shows inclusive rapidity distributions of neutrons integrated over the  $0.8^\circ$  cone for different values of  $E_T$  in the TCal. As a function of centrality, i.e., increasing  $E_T$ , a clear change in this spectrum is observed. For rather peripheral collisions the spectrum is dominated by a peak at  $y_b = 3.44$ . This component decreases strongly with increasing  $E_T$ . For the highest  $E_T$  bin, the dominant peak is shifted to lower rapidities.

To quantify the above observations and relate them to predictions of models the data are compared in Fig. 2 to calculations within the Landau-fireball model assuming full stopping.<sup>6</sup> While there is good agreement for the Al and Cu targets, for the Pb target somewhat larger transverse energies are observed experimentally. The same calculations reproduce very well<sup>6</sup> the  $E_T$  spectra and their saturation with increasing target mass in the forward hemisphere. Since  $E_T$  production from a thermalized system is an upper limit for rescattering effects involving participants, one could attribute the excess  $E_T$  observed for the Pb target to rescattering effects involving the target spectators. Clearly, this should be most relevant for the largest target nucleus and should not ex-

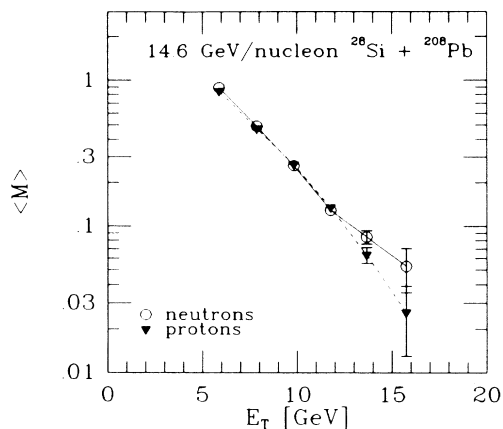


FIG. 4. Multiplicity of beam-rapidity baryons measured in a forward  $0.8^\circ$  cone as a function of transverse energy in TCal. Lines are drawn to guide the eye.

ist for Al. A similar picture emerges from a quite different approach. Figure 2 also shows results from two types of HIJET calculations for the Pb target. Without any rescattering<sup>8</sup> this model clearly underpredicts the data (dashed line with triangles). Allowing secondaries to rescatter<sup>9</sup> leads to a drastic increase in transverse-energy production into the acceptance of this experiment and the calculation now agrees well with the experimental data. For the lighter targets such rescattering effects are much smaller.

Interesting information can also be obtained by comparing predictions of the same models for the measured nucleon-rapidity spectra for the highest  $E_T$  bin. The open circles in Fig. 3 represent a HIJET<sup>9</sup> calculation for neutrons into the  $0.8^\circ$  cone and corresponding to the experimental cut in  $E_T$ . Because of the small acceptance the experimental neutron-energy threshold does not influence the calculations above  $y=1.3$  and is therefore not incorporated. There are two major components to the calculated spectrum: beam-rapidity neutrons, left over due to the finite mean free path in this model, and low-rapidity neutrons peaked near  $y=1.6$ . The low-rapidity component is very similar to the spectrum of neutrons emitted from an isotropic fireball into the same acceptance (dashed curve). The peak in the data near  $y_b=3.44$ , qualitatively reproduced by the HIJET calculations but absent in the simple fireball calculations, may reflect the very small but finite transparency of the target and is quantitatively studied in Fig. 4. Both the isotropic fireball and the HIJET model underestimate the measured cross section for neutrons in the rapidity interval  $2 < y < 3$ . The data observed in this interval are, however, consistent with what one expects from a longitudinally expanding fireball<sup>6</sup> (solid curve), where the initial pressure gradient leads to increased baryon kinetic energies.

The probability of observing a beam-rapidity neutron decreases to very small values in central collisions. This is shown in Fig. 4, where we plot the average multiplicity  $\langle M \rangle$  of beam-rapidity neutrons and protons as a function

of TCal  $E_T$ . This is obtained by integrating, above  $y=3$ ,  $d\sigma/dy$  cross sections for protons and neutrons and normalizing the cross sections to the corresponding 2-GeV bins of the  $d\sigma/dE_T$  distribution. The results for protons and neutrons agree within the statistical errors and demonstrate in a very direct way the extent of stopping in these collisions: At  $E_T=6$  GeV an average of one proton and neutron with beam rapidity survive from the 28 projectile nucleons; this number is reduced to about 0.04 for  $E_T > 15$  GeV (representing  $\frac{1}{300}$  of the reaction cross section). This implies a nuclear transparency of  $T \approx \frac{1}{350}$  and corresponding stopping probability  $p_S = 1 - T > 0.99$ . Assuming full overlap between target and projectile and interpreting this number in terms of a nucleon mean free path leads to  $\lambda \approx 1.3$  fm in the c.m. system of the participating nucleons. This is rather an upper limit since even at  $E_T=16$  GeV there may still be a contribution from not completely central collisions leading to projectile nucleons traversing substantially less target material or missing the target altogether. To settle this question of finite nuclear transparency versus impact-parameter fluctuations, data at still higher transverse energies will be needed.

In conclusion, both the transverse-energy distributions and forward-nucleon spectra measured in this experiment demonstrate quantitatively that, at AGS energies, nuclei can be fully stopped in a heavy target.

We acknowledge excellent support by the BNL AGS and Tandem staffs and thank Dr. Y. Makdisi and Dr. H. Brown for expert help in the design and running of our beam line. We would like to thank Dr. W. J. Willis for important contributions in the initial phase of this experiment and acknowledge support by CERN in the U calorimeter and TCal construction. This research is supported, in part, by the U.S. DOE, the NSF, and the Natural Science and Engineering Research Council.

<sup>(a)</sup>Present address: Physikalisches Institut, Universität, D 69 Heidelberg, Germany.

<sup>1</sup>E814 Collaboration, P. Braun-Munzinger *et al.*, *Z. Phys. C* **38**, 45 (1988).

<sup>2</sup>E802 Collaboration, L. P. Rensberg *et al.*, *Z. Phys. C* **38**, 35 (1988).

<sup>3</sup>WA80 Collaboration, S. P. Sorensen *et al.*, *Z. Phys. C* **38**, 3 (1988).

<sup>4</sup>HELIOS Collaboration, F. Corriveau *et al.*, *Z. Phys. C* **38**, 15 (1988).

<sup>5</sup>NA35 Collaboration, W. Heck *et al.*, *Z. Phys. C* **38**, 19 (1988).

<sup>6</sup>J. Stachel and P. Braun-Munzinger, *Phys. Lett. B* **216**, 1 (1989); *Nucl. Phys. A* **495**, 393c (1989).

<sup>7</sup>M. Fatyga, D. Makowiecki, and W. Llope, *Nucl. Instrum. Methods Phys. Res., Sect. A* **284**, 323 (1989).

<sup>8</sup>T. Ludlam, A. Pfoh, and A. Shor, in *Proceedings of the RHIC Workshop I, Upton, 1985*, edited by P. Haustein and C. Woody (BNL Report No. 51921).

<sup>9</sup>A. Shor and R. Longacre, *Phys. Lett. B* **218**, 100 (1989).

<sup>10</sup>R. Brun *et al.*, GEANT 3 Users Guide, CERN Data Handling Division Report No. DD/EE/84-1, 1984 (unpublished).